AFRL-AFOSR-UK-TR-2014-0033

Development of Modified Titanium Nitride Nanoparticles as Potential Contrast Material for Photoacoustic Imaging

Michael Gozin

TEL AVIV UNIVERSITY
RESEARCH AUTHORITY
RAMAT AVIV
TEL AVIV 69978 ISRAEL

EOARD Grant 13-3037

Report Date: May 2014

Final Report from 06 March 2013 to 05 March 2014

Air Force Research Laboratory
Air Force Office of Scientific Research
European Office of Aerospace Research and Development
Unit 4515, APO AE 09421-4515

REPORT DOCUMENTATION PAGE

Form Approved OMB No. 0704-0188

1. REPORT DATE *(DD-MM-YYYY)*	2. REPORT TYPE	3. DATES COVERED *(From – To)*
10 May 2014	Final Report	6 March 2013 – 5 March 2014

4. TITLE AND SUBTITLE

Development of Modified Titanium Nitride Nanoparticles as Potential Contrast Material for Photoacoustic Imaging

5a. CONTRACT NUMBER

FA8655-13-1-3037

5b. GRANT NUMBER

Grant 13-3037

5c. PROGRAM ELEMENT NUMBER

61102F

6. AUTHOR(S)

Michael Gozin

5d. PROJECT NUMBER

5d. TASK NUMBER

5e. WORK UNIT NUMBER

7. PERFORMING ORGANIZATION NAME(S) AND ADDRESS(ES)

TEL AVIV UNIVERSITY
RESEARCH AUTHORITY
RAMAT AVIV
TEL AVIV 69978 ISRAEL

8. PERFORMING ORGANIZATION REPORT NUMBER

N/A

9. SPONSORING/MONITORING AGENCY NAME(S) AND ADDRESS(ES)

EOARD
Unit 4515
APO AE 09421-4515

10. SPONSOR/MONITOR'S ACRONYM(S)

AFRL/AFOSR/IOE (EOARD)

11. SPONSOR/MONITOR'S REPORT NUMBER(S)

AFRL-AFOSR-UK-TR-2014-0033

12. DISTRIBUTION/AVAILABILITY STATEMENT

Distribution A: Approved for public release; distribution is unlimited.

13. SUPPLEMENTARY NOTES

14. ABSTRACT

The focus of this project was to develop synthetic methodologies and evaluate Titanium Nitride (TiN)-based nanomaterials, as prospective contrast agents for Photoacoustic (PA) Tomography, according to the following program:
1. Development of methodologies for preparation of stable nano-suspensions of TiN nanoparticles (TiN NPs) in physiological solution and plasma, by using natural and synthetic dispersants.
2. Development of methodologies for preparation of TiN NPs nano-suspensions based on modification of TiN NPs by molecules capable of binding to TiN NPs and having biological receptor-targeting moieties.
3. Testing stability of the receptor-targeted TiN NPs nano-suspensions in physiological solution and in plasma.
4. Evaluation of cell-binding capabilities of the receptor-targeted TiN NPs vs. non-targeted TiN NPs in relevant cellular models.

15. SUBJECT TERMS

EOARD, Nano particles, Photo-Acoustic Sensors

16. SECURITY CLASSIFICATION OF:			17. LIMITATION OF ABSTRACT	18, NUMBER OF PAGES	19a. NAME OF RESPONSIBLE PERSON
a. REPORT	b. ABSTRACT	c. THIS PAGE			James H Lawton, PhD
UNCLAS	UNCLAS	UNCLAS	SAR	17	**19b. TELEPHONE NUMBER** *(Include area code)* +44 (0)1895 616187

Development of Modified Titanium Nitride Nanoparticles as Potential Contrast Material for Photoacoustic Imaging

By: Ludmila Fadeev, Michael Shur, Michael Gozin (Tel Aviv University, Tel Aviv, Israel); Adam de la Zerda, Jesse Jokerst, Michael Mastanduno, Sanjiv Sam Gambhir (Stanford University, CA, USA); Nicole Schaeublin, Saber Hussain (AFRL, Wright Patterson AFB, Dayton, OH, USA).

Introduction

One of the most promising emerging techniques for *in vivo* medical diagnostics is a Photoacoustic Tomography (PAT). This type of tomography is a non-ionizing and a non-invasive imaging modality, based on the effect in which light is converted into ultrasound waves.[1] Photoacoustic (PA) signal is highly sensitive to absorption characteristics of the sample and pulsed laser light is required for illumination of the examined tissue or organ.[2] Absorption of focused light by a sample leads to transient variations in temperature at the area of irradiation, resulting in the generation of acoustic signals that could be measured and converted into a three-dimensional image of this area. PA imaging combines the advantages of highly sensitive optical imaging with high ultrasound resolution, capable of producing an *in vivo* three-dimensional images with very high spatial resolution (down to 50 μm) and a significant depth of penetration (up to 5 cm). Additional important aspect of PA images is that they can be reconstructed in a quantitative manner. PA imaging has been used in a number of applications, where intrinsic contrast is available, including visualizing blood vessels structure, thermal burns and melanoma.[3] However, many disorders are not showing a strong PA contrast and require the use of a contrast agent that targets the tissue of interest. Therefore, one of main challenges in this field is to develop contrast molecular agents that would produce a sufficient PA signal (in order to be detected at low concentrations), while being able to target specific tissues and organs. The ideal PA contrast agent will have a sufficiently large optical absorption cross section, to maximize the agent's PA signal, but would be small enough, to minimize uptake by the reticuloendothelial system (RES), specifically the liver and the spleen. Designing such an imaging agent is a very challenging task, since a particle's absorption cross-section and its size are highly correlated. Prospective PA contrast agents based on modified fullerenes, carbon nanotubes and gold nanoparticles (including nanocages and nanorods) were very recently reported.[4] Nevertheless, this field is still in its infancy and other much better performing materials (generating significantly stronger PA signal), capable of targeting specific tissues, are greatly needed.

Recently we discovered that TiN NPs are able to produce a very strong PA response. TiN is a non-toxic FDA-approved ceramic material, frequently used for coating of metals and alloys to improve their surface properties.[5] For example, is commonly used as a coating layer in surgical tools and medical prostheses. TiN NPs are also used as absorbent-additive material in sun energy-to-heat absorption tubes, absorbing up to 80% of the sunlight and efficiently converting it to heat. TiN NPs with average sizes relevant to potential biomedical applications are produced by Plasma Arc Vapor Synthesis method on a large scale and are commercially available from several sources. In order to obtain stable suspensions of TiN NPs in aqueous solutions for PAT, development of suitable bio-compatible dispersants was required.

Development of Serum Stable TiN NPs for Photoacoustic Tomography

During our studies with the commercially available Titanium Nitride Nanoparticles (TiN NPs; Figure 1), experiments for suspending TiN NPs in physiological media and serum were performed. The UV-vis-NIR absorption spectrum of aqueous dispersion of TiN NPs revealed the high optical absorption yields of these NPs (Figure 2). This high absorption of the material is an essential factor for obtaining a strong PA signal.

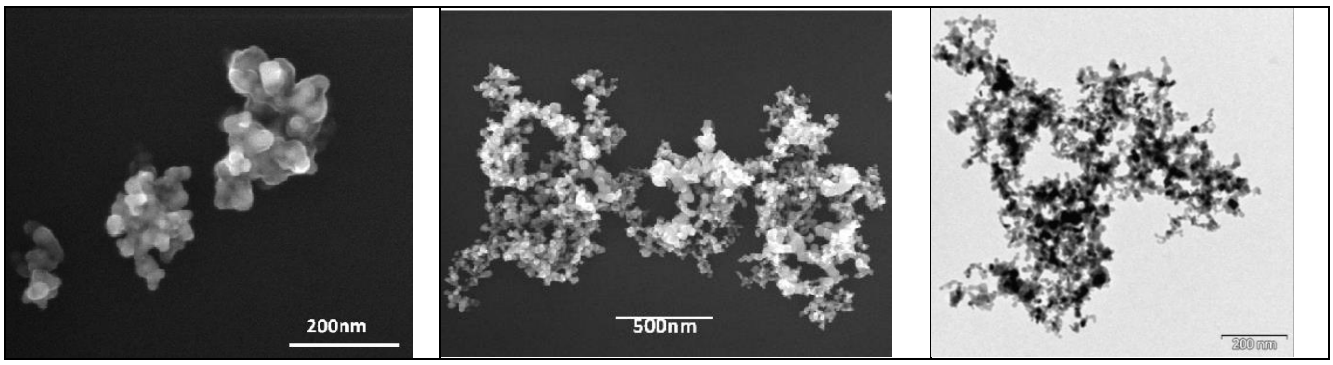

Figure 1. Images of commercially avalable TiN NPs. (*left and middle*): SEM; (*right*): TEM.

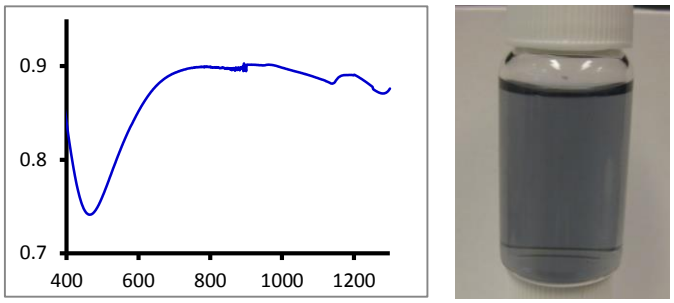

Figure 2. UV-vis-NIR absorption spectrum of TiN NPs dispersion in aqueous solution.

Once the TiN NPs were dispersed in physiological medium (1X PBS buffer, pH 7.4), the resulting dispersion was found to be somewhat unstable, showing aggregation and precipitation of the NPs. Therefore, in order to better stabilize these dispersions, various synthetic and natural stabilizing agents were used (Figure 3). Both neutral and charged dispersants were tested, however, none of them was able to successfully perform this task.

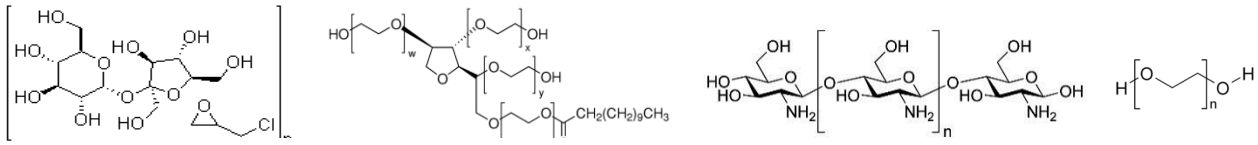

A **B** **C** **D**

Figure 3. Dispersants that were used for stabilizing TiN NPs dispersions. (*A*): Ficoll 400; (*B*): Tween 80; (*C*): Chitosan; (*D*): PEG-400.

In parallel to development of better stabilization of TiN NPs dispersions in physiological media, their potential use as PAT contrast agent was evaluated. The initial attempts were conducted using agarose-based phantom. A phantom is a polymeric material, which mimics a living tissue, for imaging purposes. The phantom was injected with Ficoll 400-TiN NPs dispersion. Additional phantom (reference) was injected with single-walled carbon nanotubes (SWCNTs), a material known for its high PA signal. It was found that the Ficoll 400-TiN NPs material was way superior to SWCNTs, exhibiting more than *30-fold stronger response* (calculated for the same concentration of the tested nanomaterial; Figure 4).

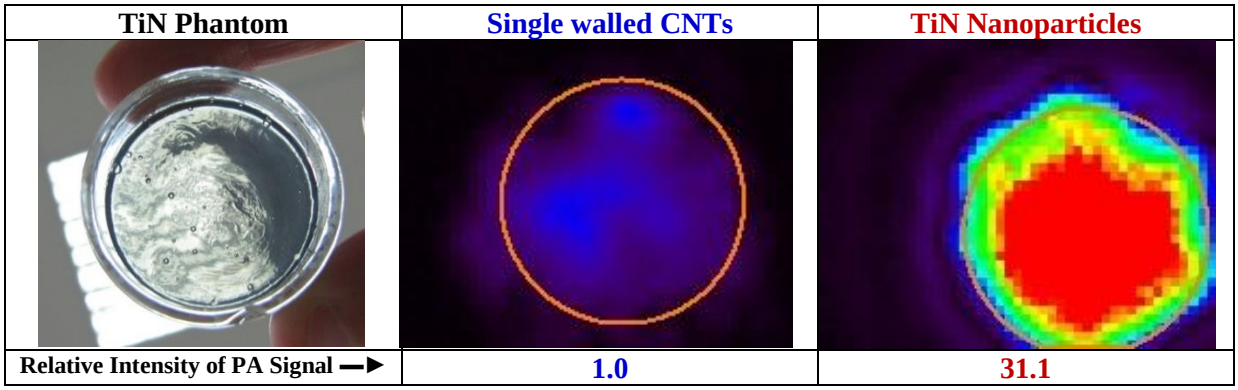

Figure 4. PA signal intensity measurements. (*left*): picture of a phantom in a glass vessel; (*middle*): PA image of the reference phantom containing SWCNTs; (*right*): PA image of phantom containing Ficoll 400-TiN NPs.

Following phantom studies, *in vivo* PAT experiment was performed in a brain tumor-bearing mouse, which was injected into its tail vein with Ficoll 400-TiN NPs dispersion. Upon injection, a very fast distribution of TiN NPs was visually observed, expressed by a significant coloration of the mouse's skin. A very strong PA signal was detected in a brain tumor tissue, allowing us to map the tumor location with very high precision and effectiveness (Figure 5).

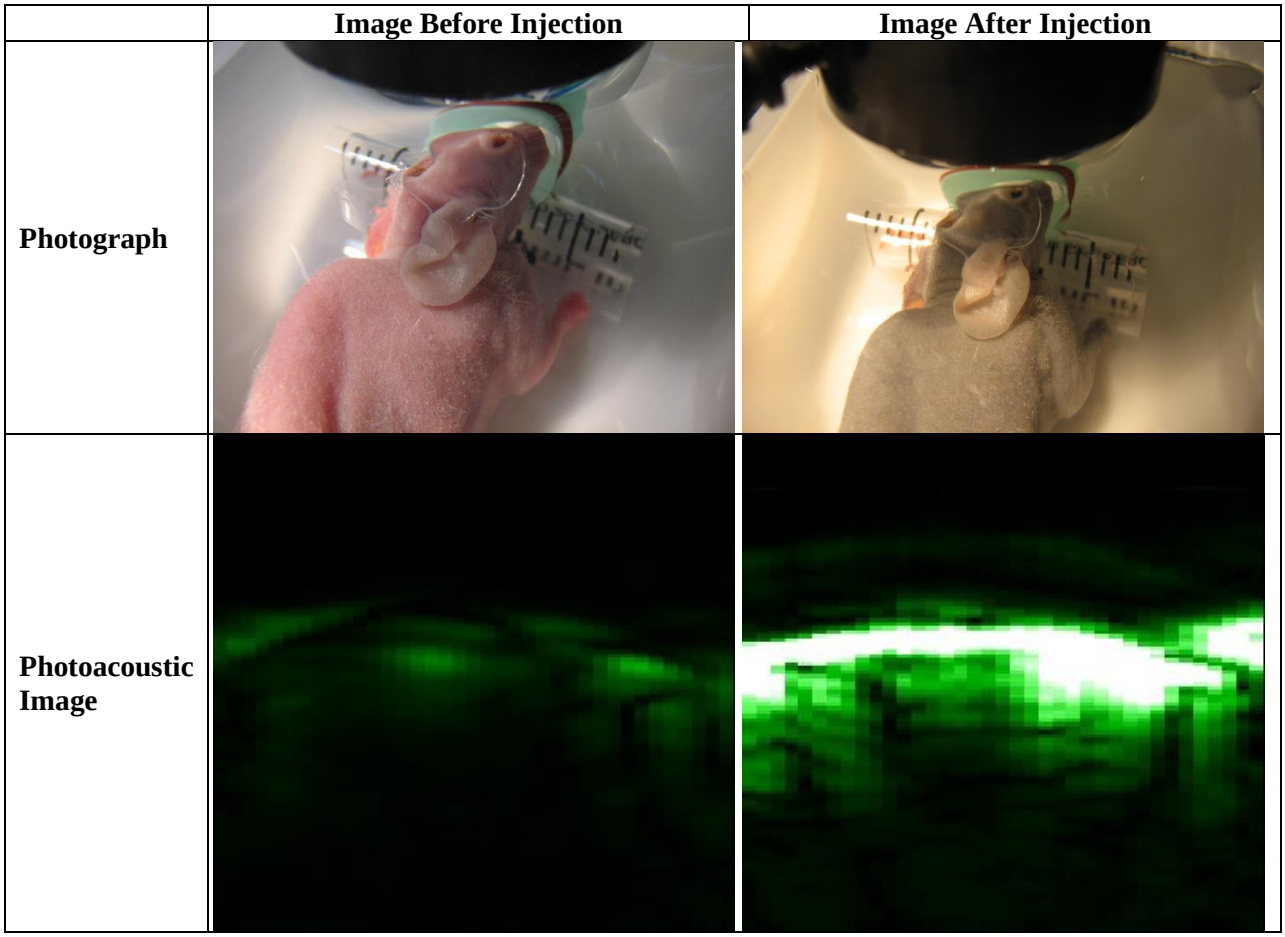

Figure 5. (*top left*): Picture of mouse with a brain tumor, positioned in a PA imaging system, *prior* to Ficoll 400-TiN NPs injection; (*top right*): PA image of a brain tumor of this mouse, *prior* to Ficoll400-TiN NPs injection; (*bottom left*): Picture of the same mouse, *after* Ficoll400-TiN NPs injection; (*bottom right*): PA image of a brain tumor, *after* Ficoll400-TiN NPs injection.

TiN NPs Characterization

The characterization effort of the TiN NPs dispersions included measurements with DLS, ζ (zeta) potential and TEM imaging. Due to the surface acidity of pristine TiN NPs, ζ potential measurements were conducted in different pH environments (Table 1).

Table 1. Pristine TiN NPs dispersion DLS and ζ potential measurements at various pHs.

pH	Buffer	Size [nm]	ζ Potential [mV]
2.0	Glycine	358 ± 32	**+21.2±1.6**
4.0	Citrate	358 ± 32	**-24.8±1.9**
5.0	Citrate	358 ± 32	**-43.4±3.3**
6.0	Citrate	358 ± 32	**-45.2±3.5**
7.0	Phosphate	358 ± 32	**-40.5±3.1**
8.0	Phosphate	358 ± 32	**-42.5±3.3**

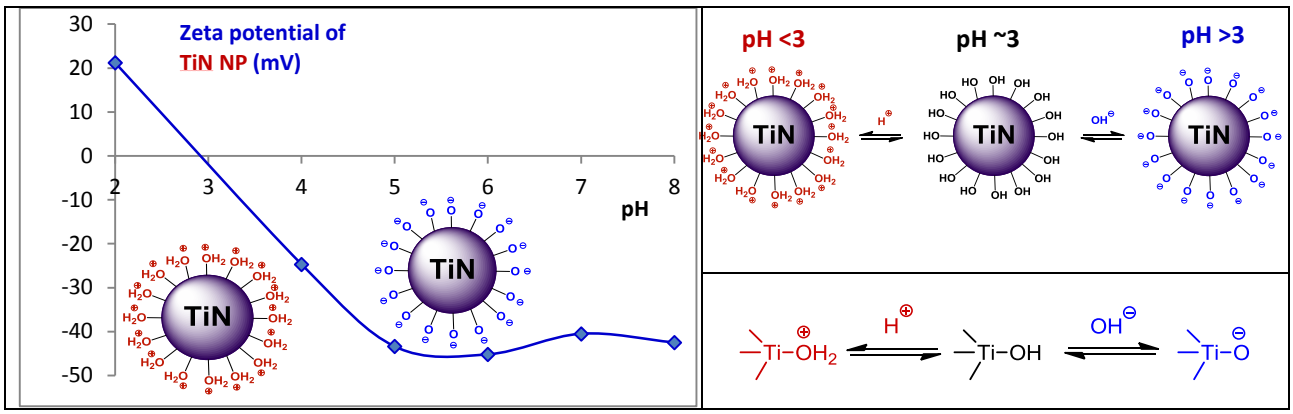

Figure 6. (*left*): Changes in ζ potential of the pristine TiN NPs dispersion as a function of pH; (right): TiN surface protonation and de-protonation mechanism.

ζ (zeta) potentials measurements revealed that the TiN NPs have an isoelectric point at around pH 5, as reported in the literature (Figure 6).[6] At pH values below 3, the Ti-OH groups on the NPs' surface are protonated and the surface is positively charged, whereas at pH values above 3, these groups are partially de-protonated, resulting in negative ζ potential values (Figures 6 and table 1).

Furthermore, TEM imaging and size measurements by DLS revealed that TiN NPs tend to aggregate, into larger clusters of few hundred nanometers in size. We hypothesized that the prevention of this aggregation could be a possible strategy for improving the TiN NPs' aqueous dispersion stability.[7]

Prevention of Aggregation

To break the TiN NPs aggregates into primary particles and possibly prevent their re-aggregation, two mechanical dispersion methods were employed.

Sonication

Ultrasonic sonication is the simplest and most widely used technique for agitation, promoting dissolution and dispersion of solids in liquid media. It is also widely used for preparation of NPs by sono-chemical processes[8] and breaking their aggregates and agglomerates into primary particles.[9] In our work, several sonication procedures were employed to assess their efficiency in reducing the size of TiN NPs' aggregates in water. Both ultrasonic bath and ultrasonic probe were used, conducting sonication procedures up to 1 hour in length. While sonication in an ultrasonic bath for 1 hour did not appear to have any detectable effect on aggregates' size, sonication with an ultrasonic probe in a polypropylene vial caused the vials melting, due to high temperatures generated as a result of the probe-sonication. None of the sonication procedures used succeeded in reducing the TiN aggregates size to the primary NPs.

Planetary Micro Ball Milling

Another common technique of grinding and breaking aggregates into primary particles is grinding and milling. Different types of the grinding and milling methods exist. For example, ball mills, roll mills, tower mills, high pressure grinding rolls and many others. The grinding of materials in all these techniques occurs due to both friction between the particles being grinded, and collisions between the particles, which apply compressive force on each other. The grinding technique which is used for grinding materials into extremely fine powders is the ball mill technique, comprised on a horizontally rotating device, partially filled with the material to be grinded, and grinding balls. The grinding balls are made of different materials with extreme hardness, such as Al_2O_3, Si_3N_4, Agate (SiO_2) and Tungsten Carbide (WC). The planetary ball mill is a ball mill capable of grinding materials into sub-micron particles, and it is frequently used in synthesis and work-up of NPs for different applications.[10] It differs from the common ball mill by using at least one grinding jar, arranged eccentrically on a wheel. The wheel rotates in opposite direction to the jar. The grinding balls in the jar are subjected to superimposed rotational movements, which produce high-energy interaction between frictional and impact forces. The Pulveristte 7 planetary ball mill was used to mill the pristine TiN NPs, with and without using grinding balls (Figure 8).

Figure 7. (*left*): Pulverisette 7 Premium Line planetary micro ball mill; (*right*): various grinding balls.

The idea behind milling TiN NPs without grinding balls was that TiN NPs will act as grinding material for itself. The milling was conducted in the presence of t-BuOH (as a solvent) in a stepwise manner. The resulted TiN NPs were characterized by DLS (Table 2).

Table 2. TiN NPs size measurements by DLS after ball milling.

Material	Milled with Balls	Milled without Balls	Not milled (reference)
TiN Particle Size	164 ± 6 nm	128 ± 1 nm	358 ± 32 nm

It was evident from the results presented in Table 2 that the ball milling technique was only partially effective in reducing the TiN NPs size. However, this technique was unable to break the aggregates into primary particles, which was our primary goal. Notably, the addition of milling balls to the milling jar did not have a positive effect. This may be due to the fact that the milling balls size and composition (Agate, 9 mm) is not the suitable material and size for grinding of TiN NPs aggregates. Better selection of milling balls would be ZrO_2 (0.1 mm), as suggested by the ball mill manufacturer. Unfortunately, ZrO_2 milling balls and the corresponding ZrO_2 milling jar were not available at the time of our research.

Preparation of Water Stable TiN NPs

As we previously demonstrated, commercially available TiN NPs were found to suffer from poor water stability, tending to aggregate and precipitate. This phenomenon is even more profound in the PBS buffer, probably due to a high ionic strength of the solution, which encourages aggregation through Coulombic interactions between the NPs. We identify the aggregation and precipitation as a critical drawback for any *in vivo* application of TiN NPs. Although TiN material is approved by FDA for surgical equipment and prosthesis coating, precipitation of TiN aggregates might cause small blood vessel clogging and other negative consequences. We therefore demonstrated few possible synthetic approaches for TiN NPs stabilization, both in water, PBS buffer and Bovine serum.

TiN NPs Stabilization by Polyelectrolyte Complexation

The surface charge of TiN NPs origins from the acidity of titanol groups on the particles' surface. It was suggested that this surface charge could be used for the NPs stabilization through electrostatic interactions between the charged titanol groups and the oppositely charged stabilizing agents. A similar approach was reported for stabilization of other ceramic NPs.[11] Possible polyelectrolyte stabilizing agents might be charged proteins, polysaccharides and inorganic ions.

Complexation of TiN NPs with Sodium triphosphate

Sodium triphosphate (TPP) is a widely used penta-anion,[12] abundant in various detergents. It also commonly utilized as preservative in seafood. TPP is FDA-approved as "Generally Recognized as Safe" (GRAS) material, and therefore was proposed by us as an excellent candidate for compelxation with TiN NPs for *in vivo* imaging applications. Mixing an aqueous dispersion of TiN NPs with TPP (at pH 2) at various TiN : TPP ratios, resulted in a shift in ζ potential values of the polyelectrolyte complex, from highly positive (un-complexed TiN NPs) to negative (Table 3).

Table 3. ζ potential measurements of TiN-TPP polyelectrolyte complexes at pH 2.

TiN:TPP Ratio	ζ Potential [mV]
2:1	-35.2±1.1
1:1	-33.8±1.8
1:2	-35.2±1.3
1:5	-24.7±0.1
1:10	-27.0±0.4

This phenomenon could be explained by the adsorption of negatively-charged TPP molecules (TPP has pK_as of 1.0, 2.0 and 2.78[13]) onto the positively-charged TiN NPs surface. Changing TiN : TPP ratios up to a certain value did not alter the ζ potential significantly, whereas mixing TiN and TPP at higher ratios of (1:5, 1:10) caused decrease in the surface charge (less negative ζ potential). This decrease is presently not well-understood and may not be significant our purposes. A possible explanation may lay in the formation of a double-layer of TPP molecules on the TiN NPs' surface. This double-layer should have somewhat different surface charge, caused by electrostatic interactions or H-bonding of TPP molecules on the outer layer with TPP molecules at the inner layer. This arrangement should result in the decrease of the charge density of the outer surface, affecting the ζ potential (Figure 8).

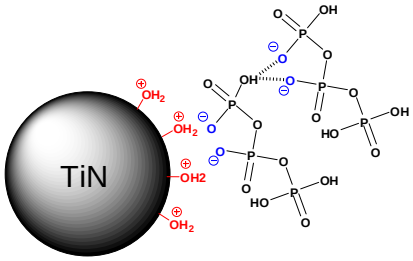

Figure 8. Proposed structure of TiN NP - TPP *double-layered* polyelectrolyte complex.

Complexation of TiN NPs with TPP and Chitosan

After the achievement of the successful complexation of TiN with TPP, we evaluated additional to TPP poly-cationic complexant – chitosan. We predicted that chitosan molecules would interact with the TPP- coated TiN NPs thorough ionic interactions. Coating of the TiN NPs with chitosan should also improve water stability through steric repulsion between neighboring NPs, as well as electrostatic repulsion between the poly-cationic chitosan chains.

Acidic chitosan solution was added to dispersions of complexes of TiN NPs with TPP (at TiN NPs : TPP ratios of 1:1 and 1:10) at [TiN NPs-TPP complex] : chitosan ratios of 1:1.6 and 1:16, in order to form an onion-like core-shell structure, containing TiN core and shells of TPP (inner shell) and chitosan (outer shell). We also prepared TiN dispersion with chitosan only, without TPP (1:1 TiN : chitosan). The resulted complexes were characterized by DLS, ζ potential (Table 4) and TEM imaging (Figure 9).

Table 4. DLS and ζ potential measurements of TiN-TPP-Chitosan polyelectrolyte complexes.

Complexes	Size [nm]	ζ Potential [mV]
TiN : Chitosan 1:1 (pH 5.5)	356 ± 25	7.6 ± 3.2
TiN : TPP : Chitosan 1:1:1.6 (pH 2)	474 ± 20	32.2 ± 0.9
TiN : TPP : Chitosan 1:10:16 (pH 2)	312 ± 15	38.5 ± 2.7

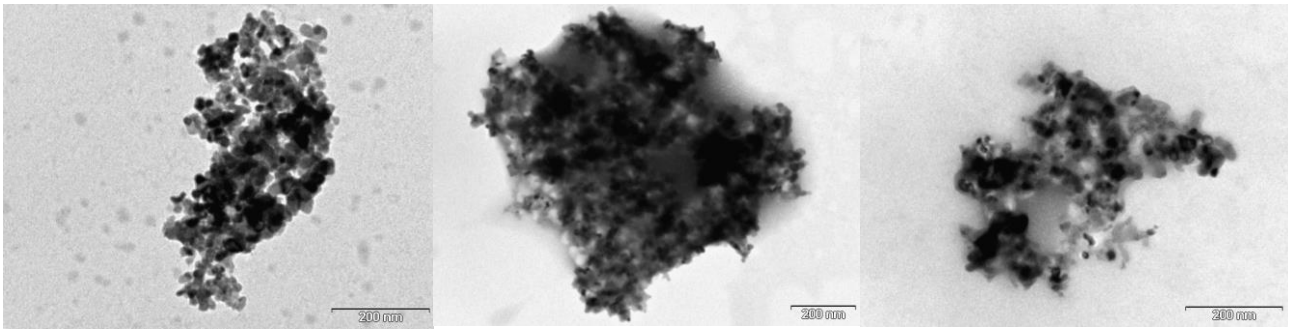

Figure 9. TEM images of TiN poly-electrolyte complexes. (*left*): TiN:Chitosan 1:1. (*middle*): TiN:TPP:Chitosan 1:1:1.6. (*right*): TiN:TPP:Chitosan 1:10:16.

Attempts of mixing pristine TiN NPs dispersion with chitosan at pH 5.5 were intended to create a coating layer of chitosan on top of TiN NPs. However, at this specific pH, both TiN and chitosan are very weakly charged and the electrostatic interactions between these two materials in aqueous media are very weak, which was demonstrated by almost neutral ζ potential value of the resulted material (7.6 ± 3.2 mV). TEM images of this material showed no presence of chitosan on top of TiN NPs (Figure 9 *left*).

Coating of TiN-TPP complexes with chitosan was found to be successful. ζ potential values of these chitosan-coated nanomaterials are highly positive (Table 4), due to the protonated amine groups of chitosan. Also, the chitosan matrix, incorporating TiN NPs, could be clearly observed from the corresponding TEM images (Figure 9 *middle* and *right*). There is a slight increase in particle size of the TiN complexes when low TiN: TPP ratio (1:1) was used, which may have a connection to the different ζ potential values that were obtained. Currently, we do not have a convincing enough explanation to the latter observation.

The various TiN complexes were tested for their stability in PBS buffer and in Fetal Bovine serum at 37°C (Figure 10).

Figure 10. (*left*): Various TiN NPs dispersions after 5 hours in serum solution at 37°C. From left to right: TiN, TiN + TPP (1:1), TiN + TPP + Chitosan (1:10:16); (*right*): the same TiN dispersions after 2 hours in PBS buffer at 37°C.

We found that both PBS and serum stability tests failed in cases of polyelectrolyte complexes of TiN NPs, as the NPs aggregated and precipitated shortly after their dispersion in the evaluated medium (Figure 10). Several explanations were proposed by us for this failure. The first one was that all the polyelectrolyte complexes, which were formed, were based on electrostatic interactions, known to be reversible and strongly dependent on the medium properties. These properties include pH, ionic strength and the nature of the present ions in solutions. It is reasonable to assume that TPP molecules, bound to TiN NPs surface, are in equilibrium with other cations present in PBS and serum. Furthermore, in PBS buffer and in serum, TiN NPs are present in their de-protonated form and are negatively charged, whereas TPP molecules are present mostly in their neutral form under these conditions. This results in a drastic decrease in the electrostatic interaction between these two species. In addition, under physiological conditions, chitosan is mostly insoluble and the fact that it is not covalently bound to TiN NPs, is probably causing its precipitation.

One also has to explain the fact that polyelectrolyte complexes of TiN NPs are much less stable in PBS buffer and in serum, as compared to un-complexed TiN NPs. If in these conditions TPP is only weakly bound to the

NPs' surface, one should expect that the NPs would be as stable as un-complexed NPs. Therefore, a change of the surface properties of the NPs is essential for causing their aggregation and precipitation.

Glycol Chitosan

The inability to use chitosan in physiological conditions due to poor solubility encouraged us to search for similar materials with improved solubility. One of the common derivatives of chitosan, which is widely used when solubility in water is desired, is glycol chitosan (Figure 11, *top left*).[14]

For polyelectrolyte complexation of TiN NPs, 5 mg of TiN NPs were added to 5 mL of glycol chitosan aqueous solution (1 mg/mL). After mixing and sonication, the resulting dispersion was tested for serum stability, revealing partial agglomeration and precipitation after a few hours. However, these results are much better than those achieved with unmodified chitosan – indicating that the insolubility of chitosan had a great effect in the instability of the dispersion.

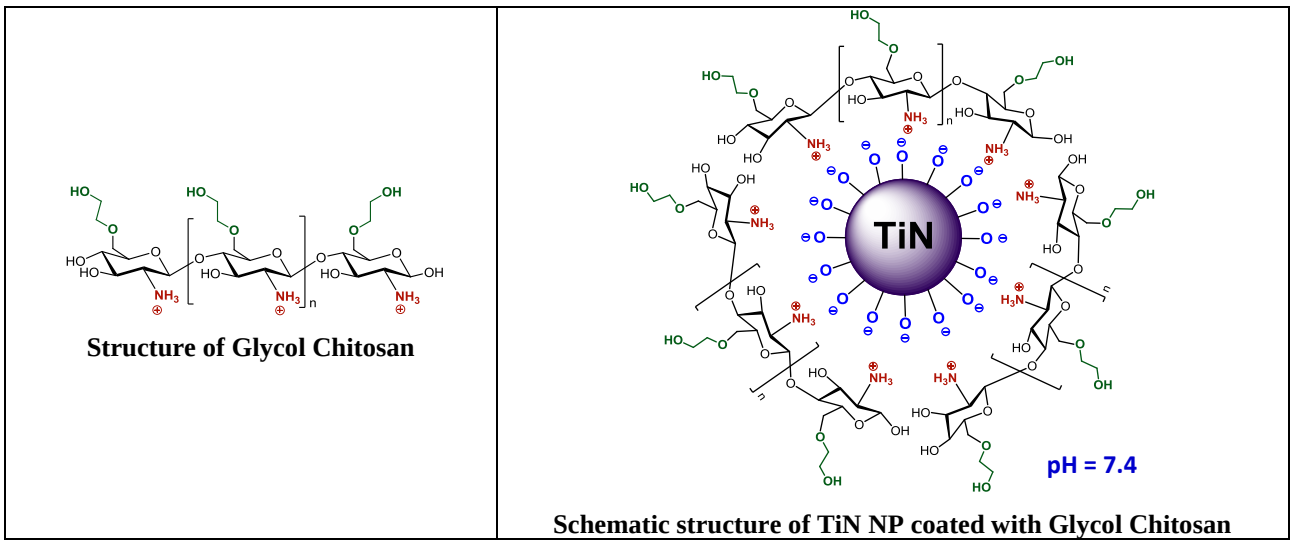

Figure 11. TiN NPs complexed with glycol chitosan – stability in serum after 3, 7 and 15 hours.

TiN NPs Stabilization by Surface Modification

Another strategy for stabilization of TiN NPs in physiological medium, which is much more promising than polyelectrolyte complexation, is chemical modification of the NPs' surface and covalent attachment of stabilizing agents. Titanol groups covering the NPs' surface might be used as anchors for chemical modification, allowing further surface modification by different bio-compatible molecules: polymers, polysaccharides and proteins. Although no literature references were found for this kind of surface modification of TiN, many reports are available on the surface modification of TiO_2 NPs,[15] which also have titanol groups on their surface. Therefore, two techniques out of those suggested for TiO_2 surface modification were employed for TiN NPs.

PEG-400

TiN NPs might be modified through surface titanol groups by etherification reaction with different alcohols.[16] This reaction should be conducted in extremely dry conditions, as traces of water will prevent the etherification reaction. We have examined modification of the NPs using PEG-400 (Figure 12).

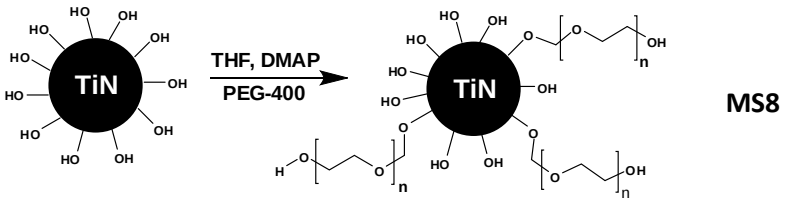

Figure 12. Synthesis of modified TiN NPs **MS8** *via* etherification.

ζ potential measurements of **MS8** modified TiN NPs reveal that the modification was not successful as the potential is similar to the un-modified TiN NPs. The reason for the failure of the modification is probably traces of water present in the PEG-400, which prevent the formation of the alkoxy intermediate of the PEG.

***N*-[3-(Trimetho-xysilyl)-propyl]ethylenediamine silane**

Another possible synthetic route for surface modification of TiN NPs is condensation reaction between the titanol groups and alkoxy-silane, similar to sol-gel chemistry reactions. Incorporation of a reactive group onto the silane may serve as an anchor for further modification. The chosen silane was *N*-[3-(trimetho-xysilyl)-propyl]ethylenediamine silane (DASi).

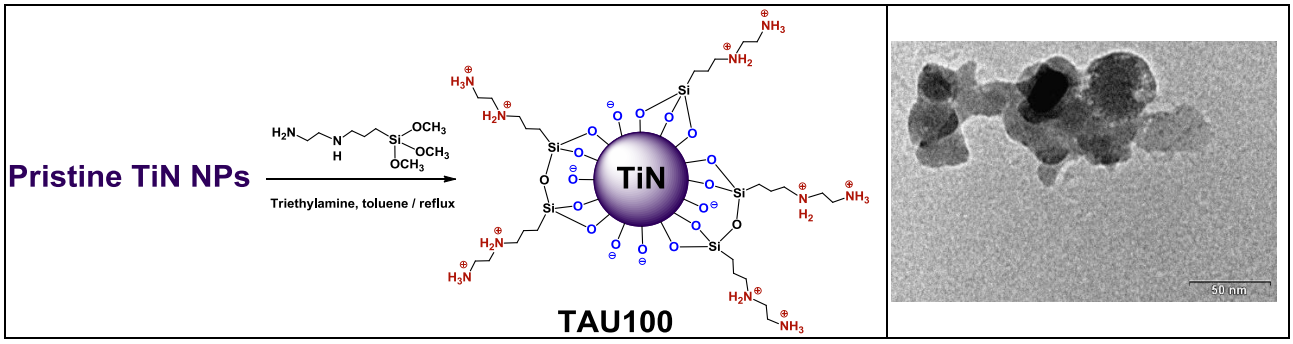

Figure 13. (*left*): Synthesis of TAU100 NPs *via* condensation reaction; (*right*): TEM image of TAU100 NPs.

DLS measurements of TAU100 NPs revealed that their average size becomes smaller (changed from 358 ± 32 nm, for pristine TiN NPs; to 208 ± 16 nm, for TAU100 NPs), where the ζ potential changed from to -24.7 ± 0.4 mV (for the unmodified TiN NPs) to +18.1 ± 0.3 mV (for TAU100 NPs), proving that the surface modification was efficient. FTIR analysis indicated presence of DASi on TiN NPs, while ζ potential of the TAU100 NPs showed "inversion" in the surface charge.

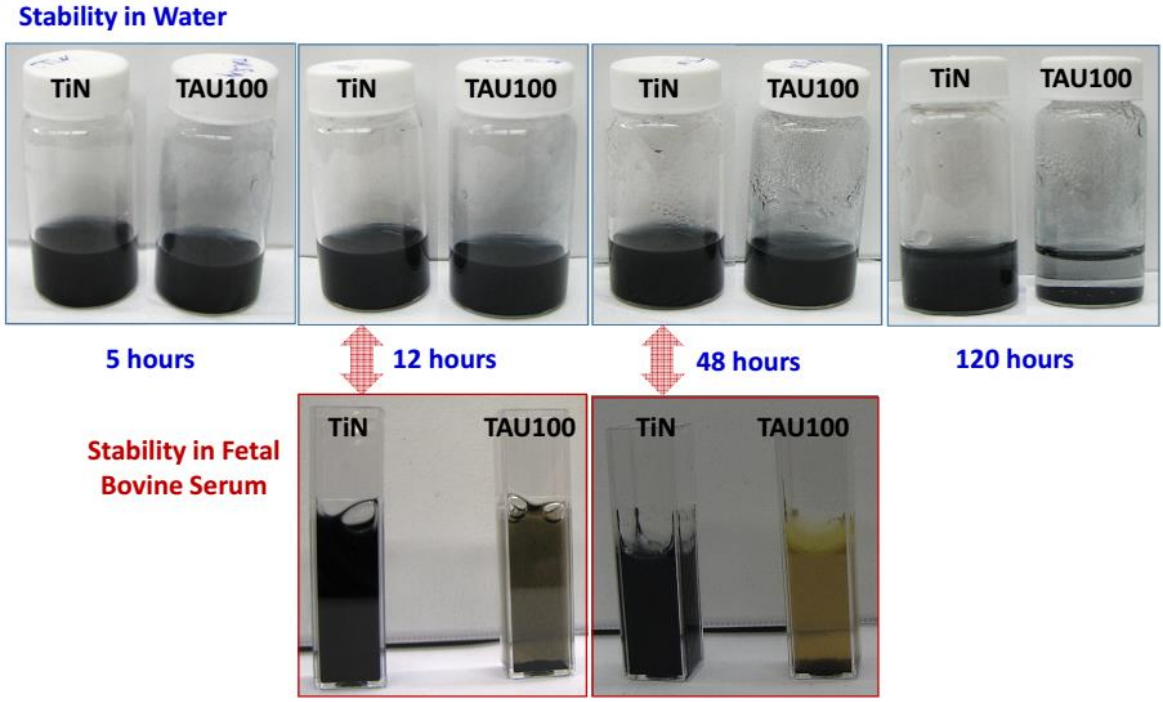

Figure 14. Dispersion stability of TAU100 NPs in water and in fetal bovine serum.

To estimate coating efficiency (number of amine groups available for further chemical reactions), we tried to attach fluorescent labels to TAU100 NPs, however, only fluorescence quenching was observed. Serum stability of the TAU100 NPs has not improved compared to the unmodified TiN NPs; TAU100 NPs were found unstable in aqueous solution and aggregate quickly (Figure 14).

It was proposed to use heparin, a polyanionic polysaccharide, in an analogous way to chitosan for the stabilization of the TAU100 NPs. TAU100 NPs (1 mg) and heparin (1 mg) were dispersed in H_2O (2 mL) by sonication, and allowed to stand for 3 days. A reference dispersion of TAU100 NPs without heparin was also prepared. The prepared complexes were characterized by DLS, ζ potential measurnments and TEM imaging. Water stability tests were also performed.

Table 5. ζ potential and DLS measurements of amino-silane modified TiN NPs in water.

Materials	Particles Size (DLS) [nm]	ζ potential [mV]
TiN NPs	358 ± 32	-24.7 ± 0.5
TAU100 NPs	208 ± 16	+18.1 ± 0.3
TAU100 NPs + Heparin	292 ± 23	-60.9±1.1

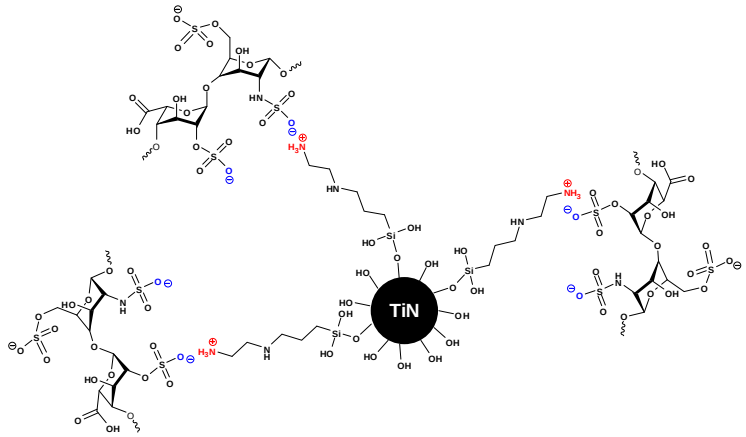

Figure 15. Proposed structure of TA100 NPs complex with heparin.

Figure 16. TAU100 NPs complexed with (*right vial*) and without (*left vial*) heparin. Their stability in H_2O after 2, 5, 12 and 24 hrs.

It can be clearly seen that comlexation of the modified TiN NPs with heparin drastically stabilizes their dispersion in water. Unfortunately, the complex with heparin turned to be unstable in serum, exhibiting aggregation and precipitation. As with chitosan, polyelectrolyte complexes are probably unstable in serum due to multiple interactions with other proteins and polysaccharides available in the medium.

We have also been able to covalently attach a protein, BSA, to the amino-silane modified TiN NPs surface. The attachment was preformed through amine groups present in BSA, using glutaraldehyde linker.[17]

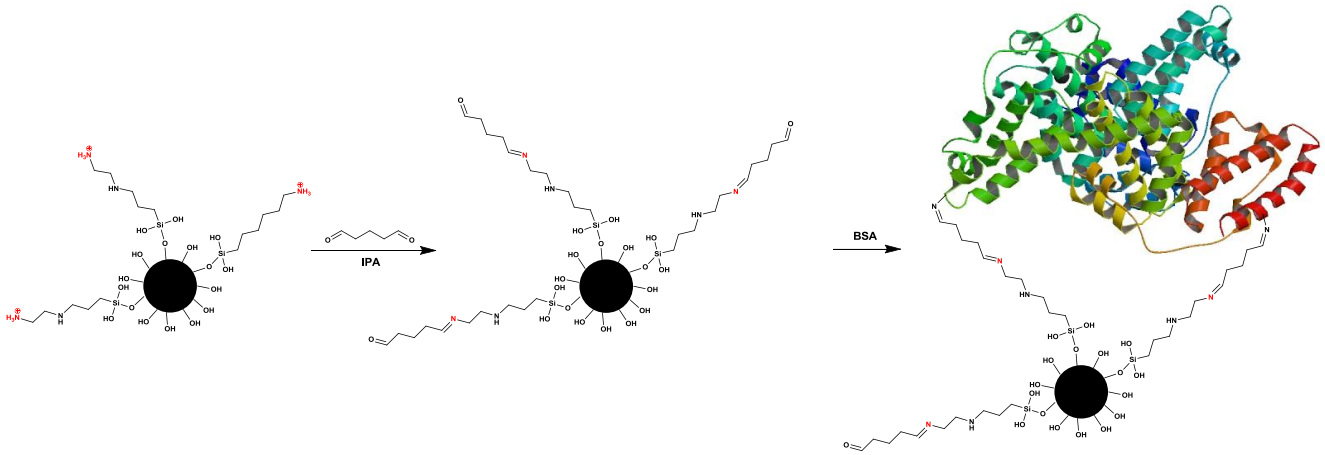

Figure 17. Synthesis of surface modification of TiN NPs with BSA (**MS10)**.

The synthesis was performed by mixing 2% aqueous glutaraldehyde solution with a dispersion of TAU100 NPs in water (1 mg/mL), followed by addition of BSA protein in 2 different methods: dropwise addition, while continuous stirring, and one-step addition. The mixture was stirred overnight, and the modified NPs were collected by centrifugation and washed with H_2O. However, NPs prepared in both methods could not be re-suspended in water, even after prolonged sonication. This was probably due to cross-linking achieved by reactions with the multiple amine groups present in BSA protein.

The unsuccessful synthesis with BSA underlines once again the need to carefully control the process of surface modification, and avoid cross-linking reactions by using mono-functional molecules throughout the synthesis. Inspired by the wide use of PEG polymers for surface modification and stabilization of NPs in the literature, we have attempted to attach covalently a CH_3O-PEG5000-COOH to TAU100 NPs.

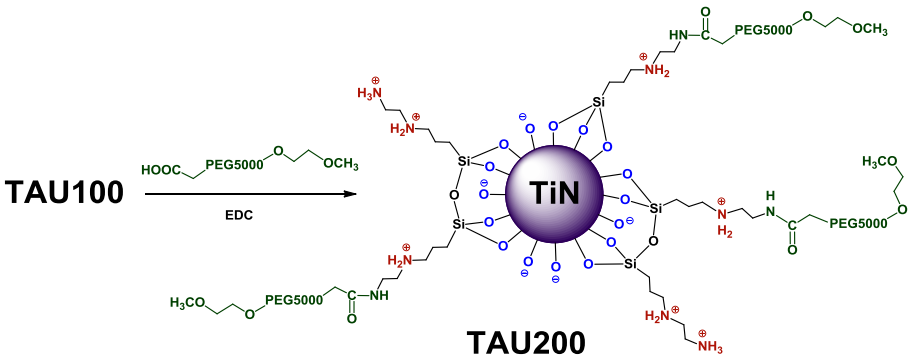

Figure 18. Synthesis of surface modification of TAU100 NPs with CH_3O-PEG5000-COOH (**TAU200** NPs).

DLS, ζ potential and other measurements were conducted to characterize the TAU200 NPs (Table 6 and Figure 19).

Table 6. ζ potential and DLS measurements of PEG - modified TiN NPs in water.

Materials	Size [nm]	ζ potential (in water) [mV]
TiN	358 ± 32	-24.7±0.4
TAU100 NPs	208 ±16	+18.1±0.3
TAU200 NPs	390 ± 48	+29.9±0.7

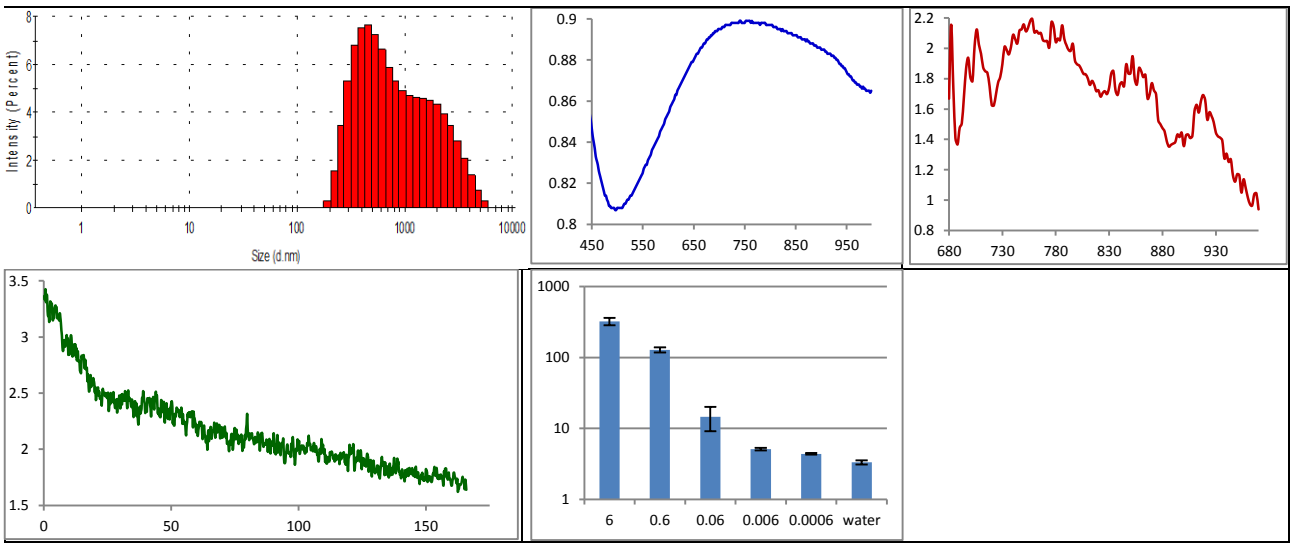

Figure 19. Analysis of TAU200 NPs. (*top left*): DLS; (*top middle*): absorbance Vis-NIR in nm, in water (0.06 mg/mL); (*top right*): photoacoustic spectrum in nm, in water (0.06 mg/mL); (*bottom left*): temporal stability results (Y-axis is the intensity of the photoacoustic signal in arbitrary units; X-axis is time in seconds); (*bottom middle*): photoacoustic signal detection limits in water (Y-axis is the intensity of the photoacoustic signal in arbitrary units; X-axis is concentration of TAU200 in mg/mL).

Serum stability test showed improvement in the TAU200 NPs stability *versus* other TiN NPs (Figure 20).

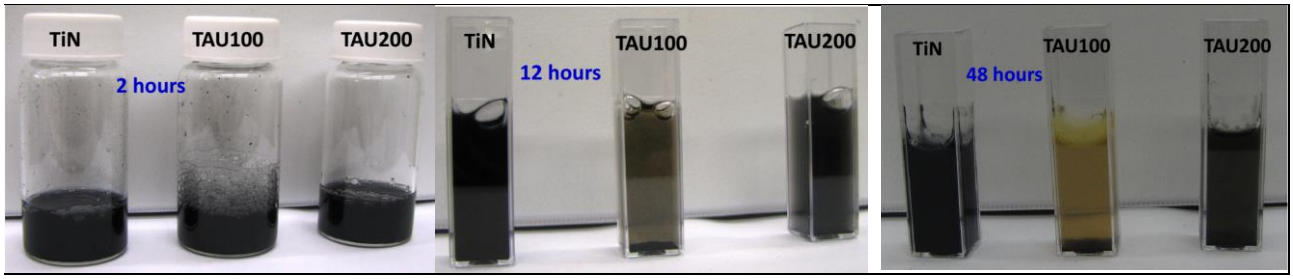

Figure 20. Dispersion stability comparison (in Fetal Bovine Serum) between parent TiN NPs, TA100 NPs and TAU200 NPs.

HaCaT Cells Uptake of Various TiN NPs – TEM and Ultra-resolution Optical Microscopy Studies

The human keratinocyte cell line (HaCaT) was generously donated by the Army Research Lab. The cells were cultured in a flask with RPMI-1640 media (ATCC, Manassas, VA), supplemented with 10% fetal bovine serum (FBS, ATCC) and 1% penicillin/streptomycin (Sigma), and incubated at 37°C in a humidified incubator with 5% CO_2. For the cytotoxicity assays, cells were cultured in 96-well plates with 2×10^4 cells per well and allowed to grow at 37°C with 5% CO_2 for 24 hrs, until ~80% confluent.

HaCaT cells were processed for TEM according to Bozzola and Russell. Briefly, the cells were seeded in 6 well plates at a density of 5×10^5 cells/well, allowed to grow overnight, until ~90% confluent, and then treated with 30 µg/mL of the various nanoparticles. 24 hrs later, the cells were removed from the plates *via* trypsin and centrifuged. The cell pellets were fixed in a mixture of 2% (w/v) paraformaldehyde (EMS Diasum) and 2.5% (w/v) gluteraldehyde (EMS Diasum) in phosphate buffered saline (PBS) for 2 hrs, then washed thoroughly with PBS, to remove any residual aldehydes, and subsequently stained with 1% (w/v) osmium tetroxide (EMS Diasum) for 1 hr. After 3 additional PBS washes, to remove any excess osmium-containing compounds, the cells were dehydrated, using increasing concentrations of ethanol, with 3 final exchanges of 100% ethanol. The samples were then placed in 100% LR White resin (EMS Diasum) and cured overnight at 60°C in BEEM capsules (EMS Diasum) in a vacuum oven. The samples were thin-sectioned on a Leica ultra-microtome at a thickness of 50-100 nm, collected on formvar/carbon-coated TEM grids and imaged using a Philips/FEI CM200 TEM at 120 kV. Controls consisted of cells not treated with nanoparticles for all experiments, unless otherwise stated.

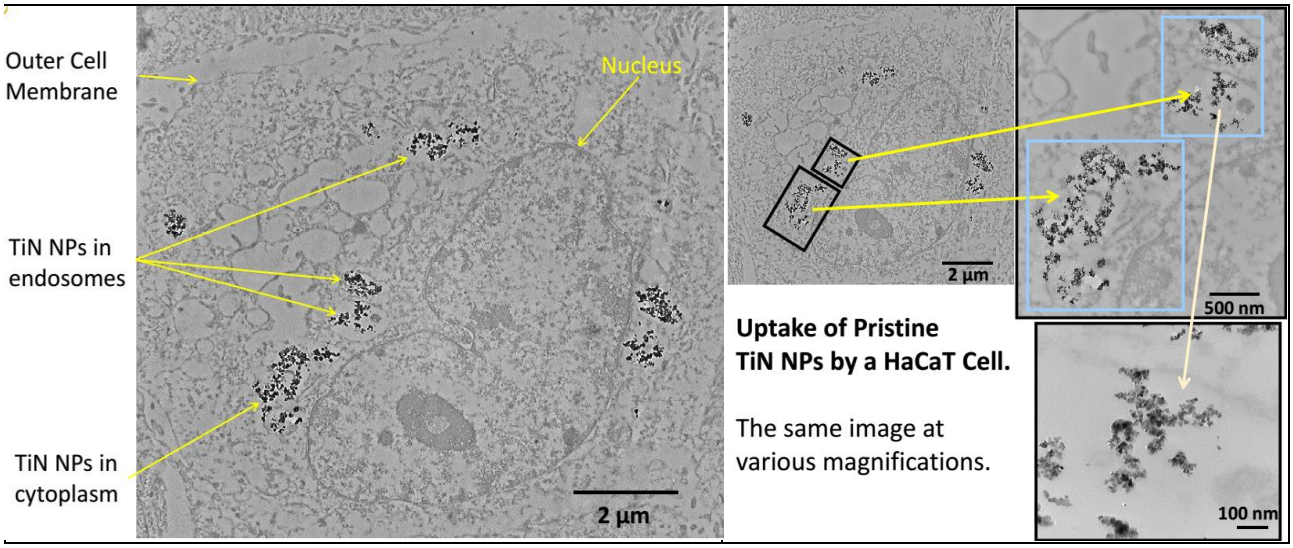

Figure 21. TEM images of pristine TiN NPs uptake by HaCaT cells.

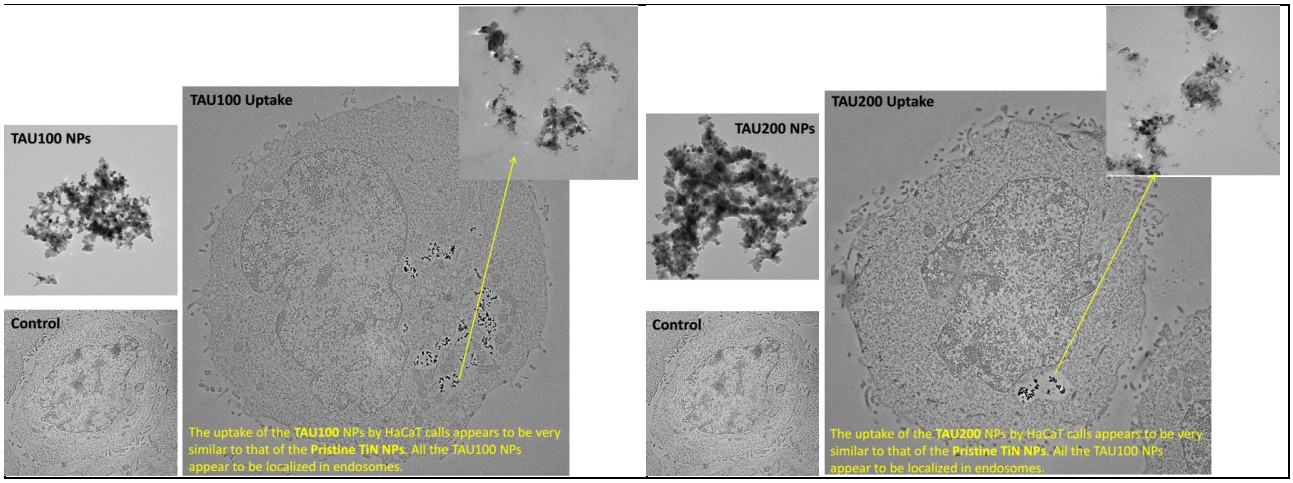

Figure 22. TEM images of TAU100 and TAU200 NPs uptake by HaCaT cells.

External Morphology and Nanoparticles Uptake by Ultra Resolution Imaging. HaCaT cells were plated on chambered slides at a density of 3×10^5 and allowed to grow at 37°C with 5% CO_2 for 24 hrs, until ~80% confluent. They were then exposed to 2.5 µg/ml of nanoparticles for 24 hrs. After exposure, the cells were fixed with 4% paraformaldehyde, stained with the Alexa 555-Phallodin and SYTOX Green (Invitrogen) stains to visualize the actin and the nucleus, respectively. The slides were mounted in Prolong AntiFade reagent (Invitrogen) and images were taken using the CytoViva 150 Ultra-resolution attachment (Aetos Technologies) to determine if the particles were taken into the cell and to observe any morphological changes (Figure 23).

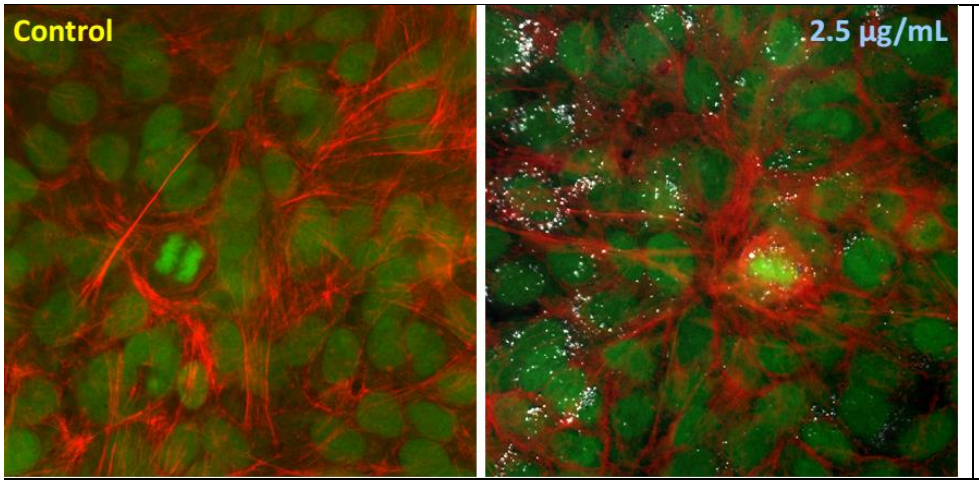

Figure 23. CytoViva 150 Ultra-resolution images of pristine TiN NPs uptake by HaCaT cells.

Mitochondrial Function

Mitochondrial function of the HaCaT cells was assessed by using the CellTiter 96 AQueous One Solution Assay (Promega). Cells were cultured in 96-well plates with 5×10^3 cells per well and allowed to grow at 37°C with 5% CO_2 for 24 hrs, until ~80 % confluent, and subsequently treated with NPs at concentrations in a range of of 0.5 to 30.0 µg/mL. After a 24 hrs exposure, mitochondrial function was assessed according to manufacturer's instructions, and as described by Braydich-Stolle. The plate was read on a SpectraMAX GeminiXS microplate reader at 490 nm, to measure the absorbance (Figure 24). Each experiment was done in a triplicate and the data are represented as the average of 3 independent experiments.

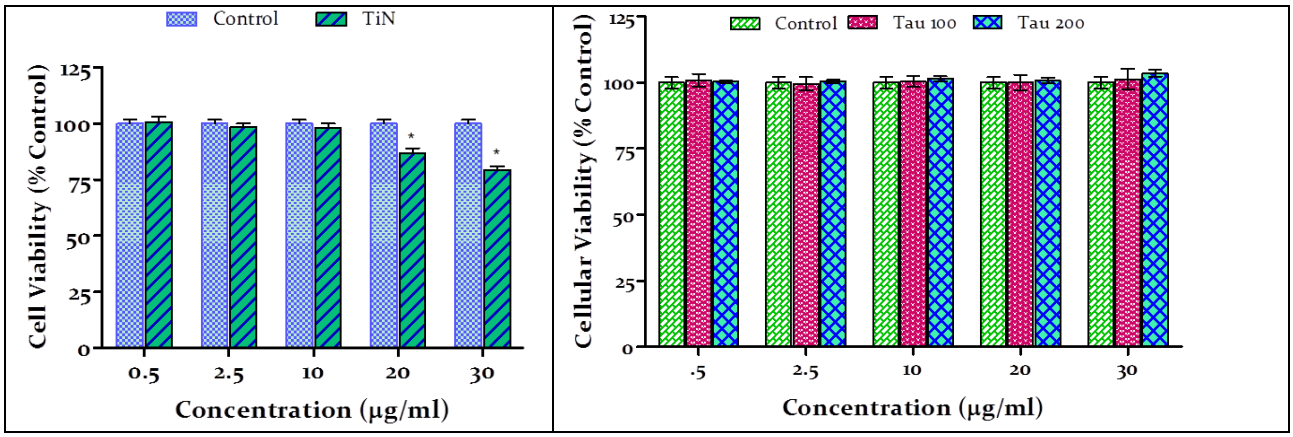

Figure 24. Results of mitochondrial function of the HaCaT cells. (*left*): The pristine TiN NPs started to cause a slight decrease in HaCaT cells viability at 20 µg/mL, while this decrease was statistically significant, about 80% of the cells were still viable after treatment with 30 µg/mL; (*right*): there was no decrease in HaCaT cells viability after exposure to TAU100 and TAU200 NPs, indicating that these NPs are not toxic up to concentration of 30 µg/mL.

Reactive Oxygen Species Generation

Prior to treatment with nanoparticles, a dichlorofluorescin diacetate probe was added and the HaCaT cells were exposed to NPs at concentrations of 0.5, 10, and 30 µg/mL. Reactive oxygen species (ROS) production was assessed following the Wang's procedure. The plate was read on a SpectraMAX GeminiXS microplate reader at a 486 nm excitation wavelength and a 530 nm emission wavelength (Figure 25).

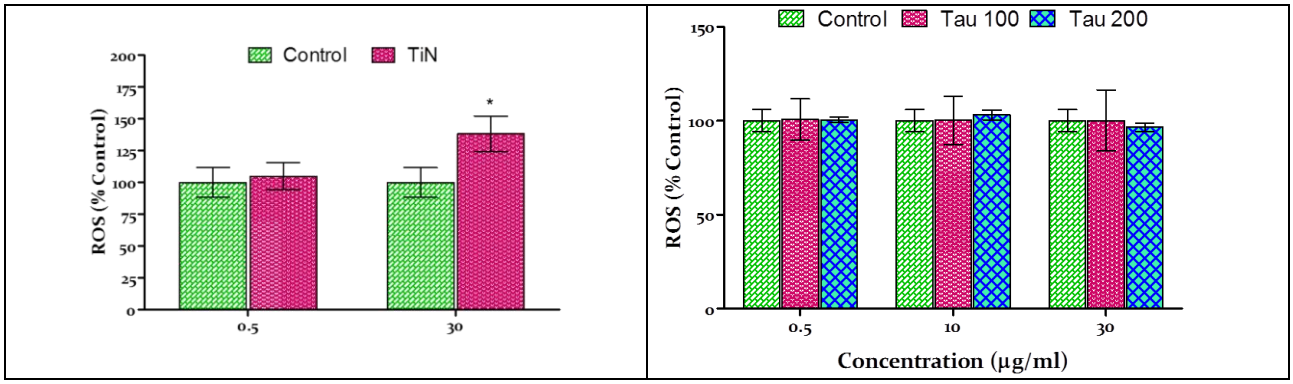

Figure 25. Results of ROS generation by NPs in the HaCaT cells. (*left*): The pristine TiN NPs cause a significant increase in ROS at 30 µg/mL. These results nicely correlate with the cells viability results and the formation of the ROS is most likely the cause of the cells death (Figure 24); (*right*): there was no decrease in HaCaT cells viability after exposure to TAU100 and TAU200 NPs, indicating that these NPs are not toxic up to concentration of 30 µg/mL.

Experimental

^{1}H NMR spectra were recorded on Bruker 400 or 500 MHz spectrometers. All NMR signals are reported in ppm. ^{1}H NMR signals are referenced to the residual proton of deuterated solvents. UV-vis spectra were measured using a Varian's Cary 5000 spectrometer. Fluorescence spectra were recorded by Jobin Yvon's spectrofluorimeter. DLS and ζ potential measurments were performed using a Zetasizer Nano Z. TEM imaging

was performed using Jeol TEM JEM 1200EX. The samples were prepared by placing a drop on a copper grid and evaporating the solvents overnight. Ball milling was performed using Pulverisette 7 (Fritsch GmbH) planetary ball mill, using Agate 9 mm milling balls.

General Procedure for TiN Milling on Pulveristte 7 Ball Mill. TiN NPs (350 mg) were dispersed in tBuOH (20 mL) and transferred into 2 Agate-made grinding jars each. 18 Agate grinding balls (9 mm) were added to one grinding jar, whereas the second jar was operated without grinding balls. The milling was conducted in 20 periods: 5 min. of grinding at 600 rpm and 7 minutes of cooling.

TAU100 NPs. TiN NPs (30 mg) were dispersed in toluene (40 mL) using sonication for 10 min. TEA (400 µL, 2.87 mmol) were added, followed by dropwise addition of *N*-[3-(trimethoxysilyl)-propyl]-ethylene-diamine silane (10 mL, 46.23 mmol). The dispersion was refluxed for 3 hrs, after which the modified TAU100 NPs were collected by centrifugation (6,000 rpm, 5 min.), washed with DCM 3 times and dried.

TAU200 NPs. CH_3O-PEG5000-COOH (5 mg, 1 mmol) and EDC-Cl (2 mg, 10.4 µmol) coupling agent were added to the dispersion of TAU100 NPs (0.5 mg/mL) and stirred for overnight. The modified TAU200 NPs were collected by centrifugation (6000 rpm, 5 minutes), washed with MeOH, to remove unreacted CH_3O-PEG5000-COOH and dried.

References

1. Karabutov, A.A.; Savateeva, E.V.; Oraevsky, A.A. Laser Physics 2003, 13(5), 711-723.
2. Ntziachristos, V.; Razansky, D. Chem. Rev. 2010, 110(5), 2783-2794.
3. Kim, C.; Cho, Eun C.; Chen, J.; Song, K. H.; Au, L.; Favazza, C.; Zhang, Q.; Cobley, C. M.; Gao, F.; Xia, Y.; Wang, L. V. ACS Nano 2010, 4(8), 4559-4564
4. de la Zerda, A.; Liu, Z.; Bodapati, S.; Teed, R.; Vaithilingam, S.; Khuri-Yakub, B.T.; Chen, X.; Dai, H.; Gambhir, S.S. Nano Lett. 2010, 10(6), 2168-2172
5. Lee, S. B.; Choi, J. Y.; Park, W. W.; Jeon, J. H.; Won, S. O.; Byun, J. Y.; Lim, S. H.; Han, S. H. Metals and Materials International 2010, 16(4), 679-686.
6. (a) Zhang, J.; Duan, L.; Jiang, D.; Lin, Q.; Iwasa, M. J. Colloid Interface Sci. 2005, 286, 209-215; (b) Guo, Z. et al. J. Alloys Compd. 2010, 493, 362-367.
7. Inkyo, M.; Tahara, T. J. Soc. Powder Tech. Jpn. 2004, 41, 578-585.
8. (a) Salkar, R. et al. J. Mater. Chem. 1999, 9, 1333-1335; (b) Fujimoto, T. et al. Chem. Mater. 2001, 13 (3), 1057-1060; (c) Kang, P. et al. Mater. Res. Bull. 2004, 39, 545-551.
9. (a) Al-Kaysi, R. et al. Langmuir 2005, 21 (17), 7990-7994; (b) Lemarchand, C. et al. Pharmaceut. Res. 2003, 20 (8), 1284-1292; (c) Sanganwar, G. P.; Gupta, R. B. Powder Technol. 2009, 196, 26-49.
10. (a) Ito, T.; Zhang, Q.;Saito, F. Powder Technol. 2004, 143-144,170-173 ; (b) Bimbo, L.M et al. Nanomaterials 2011, 32 (10), 2625-2633; (c) Suwanboon, S.; Amornpitoksuk, P.; Bangrak, P. Ceram. Int. 2011, 37 (1), 333-340; (d) Anenkova, K. A. et al. Quantum Electron. 2011, 41 (5), 393-395.
11. (a) Boddohi, S.; Moore, N.; Johnson, P. A.; Kipper, M. J. Biomacromolecules 2009, 10, 1402–1409; (b) Mori, H.; Muller, A. H. E.; Klee, J. E. J. Am. Chem. Soc., 2003, 125 (13), 3712-3713; (c) Nam, J-P.; Choi, C.; Jang, M-K.; Jeong, Y-I.; Nah, J-W. Macromol. Res. 2010, 18, 630-635; (d) Reum, N. et al. Langmuir 2010, 26 (22), 16901-16908.
12. (a) Rutkaite, R. et al. Int. J. Biol. Macromol. 2012, 50, 687-693; (b) Huang, H.; Yang, X. Biomacro-molecules 2004, 5 (6), 2340-2346.
13. Shu, X. Z.; Zhu, K. J. Eur. J. Pharm. Biopharm. 2002, 54, 235-243.
14. (a) Kwon, S. et al. Langmuir 2003, 19, 10188-10193; (b) Park, J.H et al. Biomaterials 2006 , 27, 27119-126; (c) Park, J.H. et al. J. Controlled Release 2004, 95, 579-588; (d) Lee, S. J. *et al.* Biomaterials 2009, 30, 2929-2939.
15. (a) Pietron, J. J.; Rolison, D. R. J. Non-Cryst. Solids. 2001, 285, 13-21; (b) Carrizosa, I.; Munuera, G. J. Catal. 1977, 49, 174-188; (c) Sabzi, M.; Mirabedini, S.M.; Zohuriaan-Mehr, J.; Atai, M. Prog. Org. Coat. 2009, 65, 222-228; (d) Thurnauer, C. et al. J. Phys. Chem. 1996, 100, 4538-4545
16. (a) Sun, Tao.; Yu, G.; Price, C.; Booth, C. Polymer 1995, 36, 3775-3778; (b) Kuo, P.; Kawamura, N.; Miki, M.; Okahara, M. Bull. Chem. Soc. Jpn. 1980, 53, 1689-1693; (c) Ishizu, K.; Akiyama, Y. Polymer 1997, 38, 491-494.
17. Simi, C.K.; Abraham, T.E. Colloids Surf., B 2009, 71, 319-324.